Hindawi
Journal of Nanomaterials
Volume 2017, Article ID 7460323, 9 pages
https://doi.org/10.1155/2017/7460323

Research Article

Synthesis, Characterization, and Magnetic Properties of Pure and EDTA-Capped NiO Nanosized Particles

H. T. Rahal,[1] R. Awad,[2] A. M. Abdel-Gaber,[1,3] and D. El-Said Bakeer[4]

[1]*Department of Chemistry, Faculty of Science, Beirut Arab University, Beirut, Lebanon*
[2]*Department of Physics, Faculty of Science, Beirut Arab University, Beirut, Lebanon*
[3]*Department of Chemistry, Faculty of Science, Alexandria University, P.O. Box 426, Ibrahimia, Alexandria 21321, Egypt*
[4]*Department of Physics, Faculty of Science, Damanhour University, Damanhour, Egypt*

Correspondence should be addressed to H. T. Rahal; hananrahal88@yahoo.com

Received 25 September 2016; Revised 18 November 2016; Accepted 28 November 2016; Published 15 January 2017

Academic Editor: Muhamamd A. Malik

The effect of ethylenediaminetetraacetic acid (EDTA) as a capping agent on the structure, morphology, optical, and magnetic properties of nickel oxide (NiO) nanosized particles, synthesized by coprecipitation method, was investigated. Nickel chloride hexahydrate and sodium hydroxide (NaOH) were used as precursors. The resultant nanoparticles were characterized by X-ray diffraction (XRD), transmission electron microscopy (TEM), and scanning electron microscopy (SEM). XRD patterns showed that NiO have a face-centered cubic (FCC) structure. The crystallite size, estimated by Scherrer formula, has been found in the range of 28–33 nm. It is noticed that EDTA-capped NiO nanoparticles have a smaller size than pure nanoparticles. Thus, the addition of 0.1 M capping agent EDTA can form a nucleation point for nanoparticles growth. The optical and magnetic properties were investigated by Fourier transform infrared spectroscopy (FTIR) and UV-vis absorption spectroscopy (UV) as well as electron paramagnetic resonance (EPR) and magnetization measurements. FTIR spectra indicated the presence of absorption bands in the range of 402–425 cm^{-1}, which is a common feature of NiO. EPR for NiO nanosized particles was measured at room temperature. An EPR line with g factor ≈1.9–2 is detected for NiO nanoparticles, corresponding to Ni^{2+} ions. The magnetic hysteresis of NiO nanoparticles showed that EDTA capping recovers the surface magnetization of the nanoparticles.

1. Introduction

Nanosized nickel oxide (NiO) is a significant transition metal oxide that has garnered attention as a strong candidate for many fields including superparamagnetic devices, photovoltaic devices, electrochemical supercapacitors, magnetic materials, catalysis, smart windows, fuel cell, and photovoltaic devices [1]. These nanostructured particles are regarded as a p-type semiconductor having large exciton binding energy with stable wide bandgap (3.6–4.0 eV). Bulk NiO is an antiferromagnetic insulator with a Néel temperature of 523 K [2]. They exhibit many unique magnetic, optical, electronic, and chemical properties that are significantly different than those of bulk-sized NiO particles due to their quantum size and surface effects [1].

Several methods were used to prepare NiO nanoparticles like sol-gel process [3], thermal decomposition [4], polymer-matrix assisted synthesis [5], and spray-pyrolysis [6]. Some of these techniques suffer from the difficulty in size homogeneity and dispersion of NiO nanoparticles. Generally, most techniques aim to reduce the costs of chemical synthesis and to produce materials for technological applications. However, in solution-based chemical methods for nanoparticles synthesis, a capping agent is generally added to control the size as well as the shape of nanoparticles and to prevent agglomeration of the synthesized particles. Many kinds of organic compounds such as surfactants and polymers have been used to direct or confine anisotropic growth. These capping reagents can bind with the various crystallographic surfaces to alter their growth rates [7].

Several researches have synthesized capped NiO nanoparticles using various techniques with different capping agents. Nowsath Rifaya et al. [8] synthesized nanostructured NiO particles through a simple, novel, and cost-effective chemical capping method using nickel chloride, alanine, ethanol, and ammonia. Alanine has served as capping molecule and blocked the active sites at growing surfaces. It was found that the resultant nanoparticles will be biocompatible in nature and very useful for biosensor related applications. Moreover, Davar et al. [9] synthesized NiO nanoparticles using thermal decomposition of [bis(2-hydroxyacetophenato)nickel(II)] in oleylamine surfactant. The development of such surfactant was to control nanocrystal size, shape, and distribution size. Also, nickel oxide nanoparticles (25 nm) have been synthesized by Fereshteh et al. [10] via decomposition of a new precursor nickel octanoate $Ni(octa)_2$ in the presence of oleylamine ($C_{18}H_{37}N$) and triphenylphosphine ($C_{18}H_{15}P$), in mild conditions. To control the particle size and morphology, combination of $C_{18}H_{37}N$ and $C_{18}H_{15}P$ were applied as surfactants. They play an important role in preventing aggregation of NiO. Babu et al. [11] prepared cubic phase of NiO nanoparticles with an average size of 25 nm by microwave synthesis method using citric acid as a capping agent. The observed TEM images demonstrated that NiO-CA produces nanoparticles having average size of 25 nm.

Among various types of stabilizers used for the preparation of nanoparticles, the water soluble polymer such as ethylenediaminetetraacetic acid, abbreviated as EDTA, has significant importance. EDTA has proved its efficiency in controlling the size and morphology of synthesized nanoparticles [12, 13]. Reddy et al. [14] synthesized $Zn_{1-x}Cr_xS$ (x = 0.00, 0.005, 0.01, 0.02, and 0.03) nanoparticles through chemical coprecipitation method using EDTA as a capping agent. It was found that the produced nanoparticles were sterically stabilized by EDTA. Also, Sadjadi and Khalilzadegan [15] reported the synthesis of EDTA-capped and ethylene glycol EG-capped CdS nanoparticles separately. The XRD analysis revealed formation of hexagonal form when we used EDTA as a surfactant agent, whereas a face-centered cubic structure was obtained by using EG as surfactant agent. It was found that EDTA-capped nanoparticles exhibit smaller crystal size than EG-capped particles. Devi and Singh [16] prepared nanoparticles of Eu^{3+} doped YPO_4 by coprecipitation method. Trisodium citrate dihydrate and EDTA were used as a complexing agent. With the addition of citrate and EDTA, there is a slight shift towards the lower wavelength in emission peaks. A broad peak at 250 nm is observed due to the Eu-O charge transfer band in the excitation spectra. Emission intensity decreases with complexing agent because of decrease of particle size as well as decrease of number of Eu^{3+} activators per unit volume.

This work aims to synthesize pure and EDTA-capped NiO nanosized particles by a simple low cost method, the coprecipitation method, at 500°C. Structural, compositional, morphological, optical, and magnetic studies of the prepared samples were carried out by X-ray diffraction (XRD), transmission electron microscopy (TEM), Fourier transform infrared (FTIR), UV-visible spectra, EPR, and magnetization techniques to determine the optimum conditions for preparing well-nanosized NiO particles.

2. Experimental Techniques

2.1. NiO Nanoparticles Preparation. EDTA-capped NiO nanoparticles were prepared using coprecipitation method. Nickel chloride hexahydrate $NiCl_2{\cdot}6H_2O$ (1 M), ethylenediaminetetraacetic acid, abbreviated as EDTA ($C_{10}H_{16}N_2O_8$) (0.1 M), and an alkali solution of 4.0 M sodium hydroxide (NaOH) as starting materials and distilled water as dispersing solvent were used to prepare NiO nanoparticles. 1 M nickel chloride hexahydrate ($NiCl_2{\cdot}6H_2O$) and 0.1 M EDTA were prepared by dissolution of 30 g nickel chloride ($NiCl_2{\cdot}6H_2O$, ≥98%, Sigma Aldrich) and 3.72 g ethylenediaminetetraacetic acid ($C_{10}H_{16}N_2O_8$, 95%, Sigma Aldrich) into 126 ml distilled water, respectively. The obtained solution was magnetically stirred at room temperature and a certain volume of 4 M NaOH was added dropwise to the solution to adjust its pH to 12. The final pH of the mixture was fixed to ≈12, a highly basic condition, which is convenient for the direct preparation of NiO crystals. The reaction was stirred for 2 h at 60°C. Afterwards, the resultant green product was washed thoroughly with distilled water for removal of reaction residues until the pH is 7 and then dried at 90°C for 24 h in air. Then, the dried ingots were separated and heated at 500°C for 5 h. Due to this annelation the color of the resultant powder changes from green to black.

The same procedure was applied to prepare pure NiO particles free from 3.72 g EDTA at the same annealing temperature.

Thus NiO nanoparticles were fabricated by chemical reaction as follows [17]:

$$\begin{aligned} &NiCl_2 \cdot 6H_2O + H_2O + 2NaOH \\ &\longrightarrow NiO + 8H_2O + 2NaCl. \end{aligned} \tag{1}$$

2.2. Nanoparticles Characterization. X-ray diffraction (XRD) patterns of pure and EDTA-capped NiO nanoparticles were obtained using the Bruker D8 advance powder diffractometer with Cu-Kα radiation (λ = 1.54056 Å) in the range of $10^\circ \leq 2\theta \leq 80^\circ$. Transmission electron microscopy (TEM) was applied to study the morphology and crystalline size of NiO nanoparticles using Jeol transmission electron microscope JEM 100CX, operated at 80 kV. The samples were examined using scanning electron microscope (SEM) with the objective of determining the particle shape. SEM images for pure and EDTA-capped NiO nanoparticles were performed on ASC-2100 from Serene Technology, Korea, with 20 kV. The FTIR analysis was carried by FTIR 8400S Shimadzu. The optical studies were measured using the ultraviolet-visible-near infrared (NIR) spectrophotometer V-670 that measures the absorption spectra at a wavelength of 4000 nm–350 nm at room temperature. A vibrating sample magnetometer (VSM), Lakeshore 7410, was used to investigate the magnetic properties of nickel oxide nanoparticles. The EPR spectra were performed at room temperature using a Bruker Elexsys 500 EPR spectrometer operating at the X-band frequency

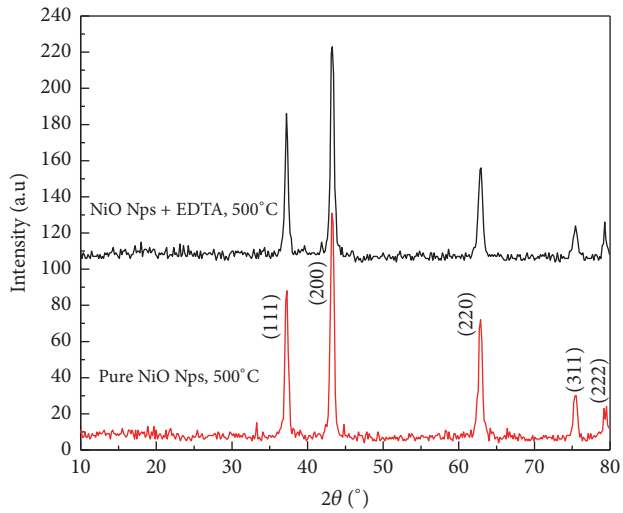

Figure 1: X-ray diffraction patterns for NiO Nps in the absence and presence of EDTA at 500°C.

(≈9.491 GHz) with a field modulation frequency of 100 kHz. The magnetic field was scanned in the range of 500–6500 G and the used microwave power was 0.64 mW. A powder sample of 100 mg was taken in a quartz tube for EPR measurements.

3. Results and Discussion

3.1. X-Ray Diffraction Patterns. Figure 1 displays the X-ray diffraction patterns for pure and EDTA-capped NiO nanoparticles annealed at 500°C. Both XRD spectra revealed the formation of face-centered cubic (FCC) NiO (JCPDS card number 47-1049) with space group Fm3hm ([225]) [18]. The five dominant diffraction peaks at approximately $2\theta = 37.34^\circ$, 43.32°, 62.9°, 75.4°, and 79.39° can be perfectly related to (111), (200), (220), (311), and (222) crystal planes, respectively. There are no peaks obtained for capping agent EDTA or Ni indicating that the nanocrystalline NiO obtained via this method consists of ultrapure phase without impurities. The sharpness and the intensity of the peaks are quite an indication of the well crystalline nature of the prepared nanoparticles. These results confirm that at 500°C the starting materials were decomposed completely to NiO. Similar patterns were observed by Gondal et al. for NiO particles prepared by pulsed laser ablation technique [19]. The lattice constant a of NiO can be calculated for prominent peak (111) using Bragg's equation:

$$a = d_{hkl}\sqrt{h^2 + k^2 + l^2}, \tag{2}$$

where (h, k, l) are the miller indices. The value of lattice constant for (111) plane was found to be 0.417 nm for both pure and EDTA-capped NiO nanoparticles. This value is very close to that for bulk NiO taken from (JCPDS card number 04-0835), which confirms the well growth of NiO. It is noted that the addition of EDTA has no effect neither on the positions of main NiO peaks nor the lattice constant

Table 1: Variation of crystalline size, optical, and magnetic properties of pure and EDTA-capped NiO nanosized particles.

Parameter	Nanoparticles	
	Pure NiO	EDTA-capped NiO
Lattice parameter a (nm)	4.174	4.171
Size (nm)		
XRD	32.65	28.314
TEM	28.775	24.631
g-value	1.92	2.09
ΔH_{pp} (gauss)	725.06	678.80
H_r (gauss)	3437.33	3153.86
$(T_2) \times 10^{-11}$ (sec)	4.71	4.62
M_r (emu/g)	4.6838×10^{-3}	4.7155×10^{-3}
M_s (emu/g)	0.22608	0.23161
H_c (G)	334.50	278.99
S	0.0207	0.0203

a. The average crystalline size (D) of the NiO particles was estimated from the line broadening measurement [20].

$$D = \frac{k\lambda}{\beta \cos\theta}, \tag{3}$$

where $\lambda = 1.54056$ nm is the wavelength of the X-ray, β = FWHM (full width at half maximum), θ is diffraction angle obtained from 2θ values corresponding to maximum intensity peak in XRD pattern (200), and k is an empirical constant equal to 0.9. The average crystalline size with the lattice constant a of pure and EDTA-capped NiO nanosized particles were calculated and listed in Table 1.

It is clearly noted from Table 1 that EDTA-capped NiO nanoparticles have smaller crystalline size than pure NiO nanoparticles. Thus, the addition of 0.1 M capping agent EDTA prevents the agglomeration of nanoparticles and forms a nucleation point for their growth [21].

3.2. Transmission Electron Microscopy. Figures 2(a) and 2(b) show the TEM images of pure and EDTA-capped NiO nanoparticles at 500°C. As seen, the uniform NiO nanoparticles with narrow size distribution and sphere shapes with weak agglomeration are obtained [22]. Most of the particle sizes are less than 40 nm. The dispersed particles in the TEM image reveal that the coprecipitation method used in this work can be considered appropriate for preparation of nickel oxide nanosized particles. One of the key factors for this desired result is the use of the capping agent EDTA, resulting in significant size reduction of nanoparticles contributing to their stability. A mechanism involves formation of strong covalent bond between polymeric chains and surfaces of nanoparticles that is responsible for stearic hindrance by which nanoparticles remain stable for months [23, 24]. Crystalline sizes obtained from TEM images are presented in Table 1. The tabulated data of the particle sizes obtained from TEM is well matched with those measured from the XRD peak broadenings.

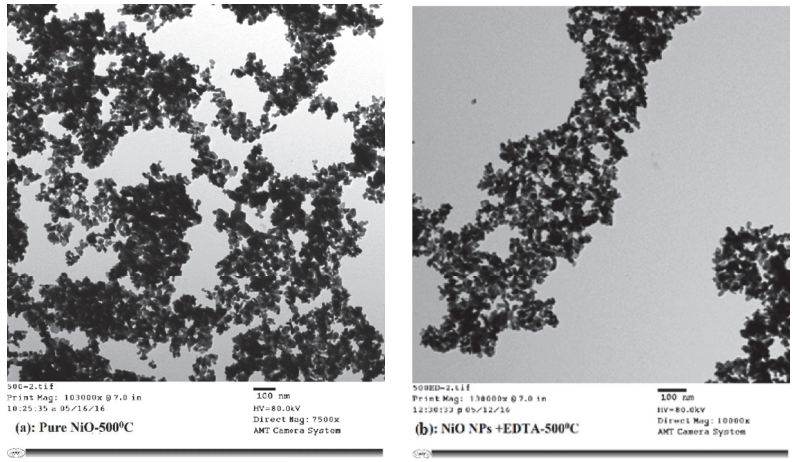

(a) (b)

Figure 2: TEM images for pure and EDTA-capped NiO nanoparticles at 500°C.

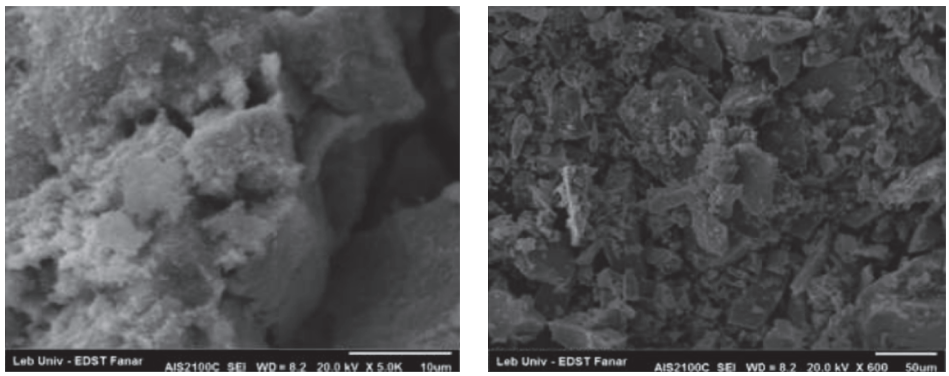

(a) (b)

Figure 3: SEM images for pure and EDTA-capped NiO nanoparticles at 500°C.

3.3. SEM Micrographs. Figures 3(a) and 3(b) show high resolution SEM images of pure and EDTA-capped NiO nanoparticles at 500°C. NiO exhibits a three-dimensional network of randomly oriented sheet-like structures. As seen from the figure, the addition of EDTA, the capping agent, controls the size as well as the shape of nanoparticles and prevents their agglomeration.

It was noted that particle shapes and sizes estimated from TEM images are rather smaller than those estimated from SEM images. TEM does not clarify the formation of NiO nanosheets.

This difference is probably due to the fact that the samples for TEM measurements were prepared from reaction solution and not from powder as in SEM. At this point, aging conditions play a decisive role in the particles sizes. Particle sizes in reaction solution are susceptible to aging effects that alter their morphological shapes.

3.4. Capping Mechanism. Figure 4 shows the interaction of the EDTA reaction sites with Ni^{2+} ion of the nickel chloride in the solution. In this mechanism, nickel chloride hexahydrate reacts with NaOH, and then it yields pure NiO nanoparticles.

Further, pure NiO nanoparticles react with EDTA $[C_{10}H_{16}N_2O_8]$ and it formed a Ni-EDTA complex ion. Such capping of NiO nanoparticles with ethylenediaminetetraacetic acid prevents their agglomeration and controls their shape and morphology resulting in lower size than pure NiO nanoparticles as depicted by XRD and TEM.

3.5. FTIR Spectra Analysis. Figure 5 reveals the FTIR spectra of pure and EDTA-capped NiO nanoparticles at 500°C. The spectra were recorded in the range of 4000 cm^{-1}–350 cm^{-1}. Both spectra display various significant absorption peaks. In both spectra, broad absorption band centered at 3440–3459 cm^{-1} is attributed to the O–H stretching vibrations band and the weak band near 1630 cm^{-1} is assigned to H–O–H bending vibrations mode. The appearance of such bands is representative of adsorbed water molecules on the external surface of NiO samples during handling to record FTIR spectra. These observations provided the evidence of the

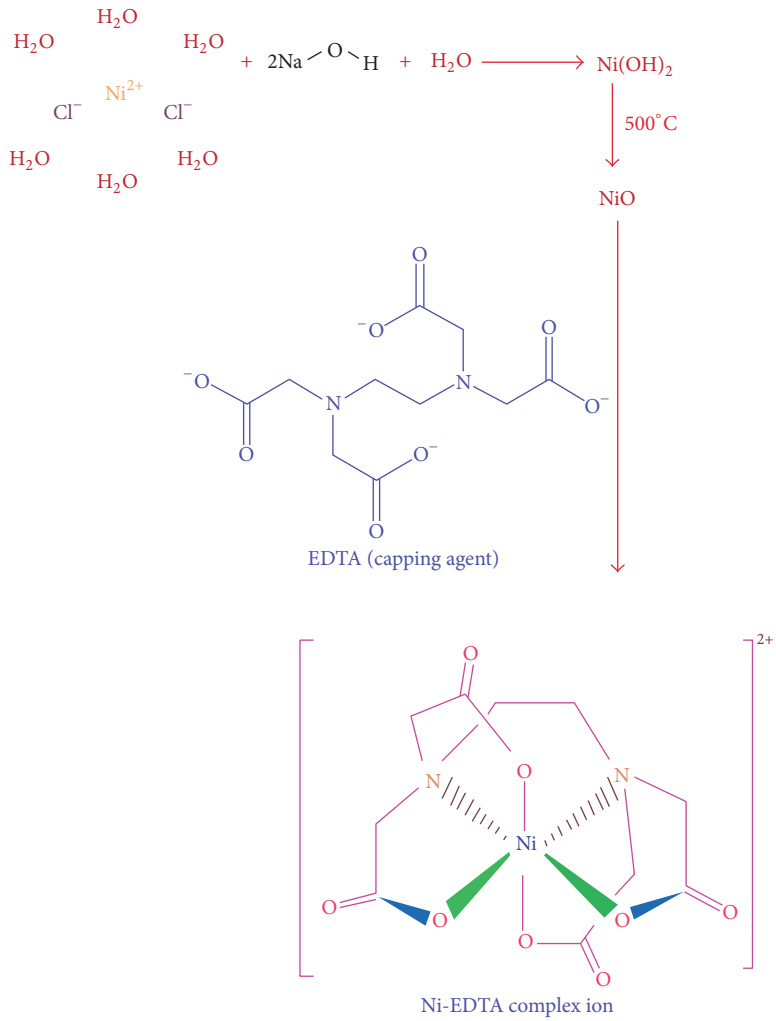

Figure 4: Ni^{2+}-EDTA complex.

effect of hydration NiO nanoparticles. The absorption bands in the region of 1000–1500 cm^{-1} are assigned to the O–symmetric and asymmetric stretching vibrations and the C–O stretching vibration [25]. The broad peak at about 402–425 cm^{-1} is assigned to stretching mode of NiO, which is clear evidence about the presence of the crystalline NiO [24, 26]. Moreover, the broadness of this band suggests that the NiO powders are nanocrystals [24]. The presence of a band in the region of 1120 cm^{-1} in EDTA-capped nanoparticles spectrum may be attributed to bending bonds which result to coordinate bonding between EDTA and Ni^{2+} indicating capping on NiO nanoparticles. It is clearly observed that the addition of EDTA does not modify or alter the position of peaks in the IR spectra of NiO nanoparticles.

3.6. UV-Vis Spectra. Figure 6 shows the optical absorption spectra of pure and EDTA-capped NiO nanoparticles at 500°C obtained by ultrasonic dispersion in absolute ethanol. The absorption edge is observed in the range of 280–350 nm [17]. The absorption peaks of NiO nanoparticles show a blue shift which may be attributed to the change in crystallite size of nanoparticles, morphology, quantum confinement of the particles, and surface effects [17]. The energy bandgaps (E_g) of the samples are calculated using the theoretical relation between the coefficient of absorption (α) and the energy of the photon ($h\nu$) as follows:

$$(\alpha h\nu)^{1/n} = A\left(h\nu - E_g\right), \tag{4}$$

where A is a constant, E_g is the energy bandgap of the material, and exponent n depends on the type of the transition. For direct and allowed transition $n = 1/2$; for indirect transition $n = 2$ and for direct forbidden transition $n = 3/2$.

Energy bandgap E_g was obtained using the intercept of the linear portion of the curve $(\alpha h\nu)^2$ versus $h\nu$ to $y = 0$ as shown in Figure 7. The obtained energy gap was found to be 3.085 eV for pure NiO and 3.116 eV for EDTA-capped NiO nanoparticles. Such increase in the bandgap may be attributed to the quantum confinement effect created by EDTA surfactant [15, 27–29]. The resultant values of E_g of NiO nanoparticles are found to be less than that obtained in literature [30]; this may be due to the preparation method used. Khalaji and Das [30] synthesized nickel oxides

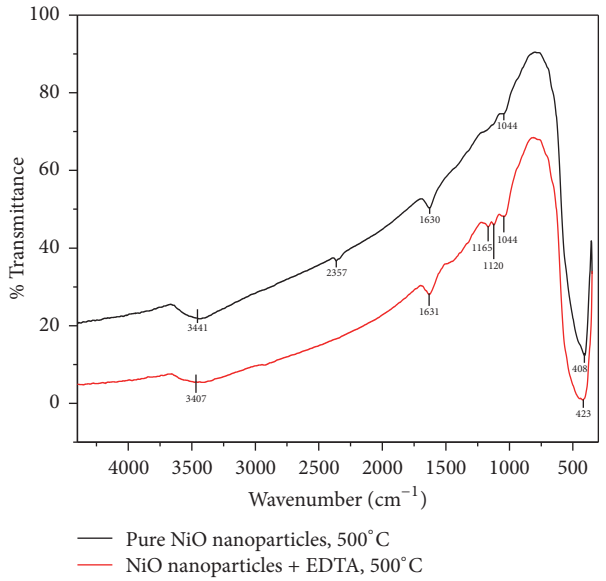

Figure 5: FTIR spectrum of pure and EDTA-capped NiO nanoparticles at room temperature.

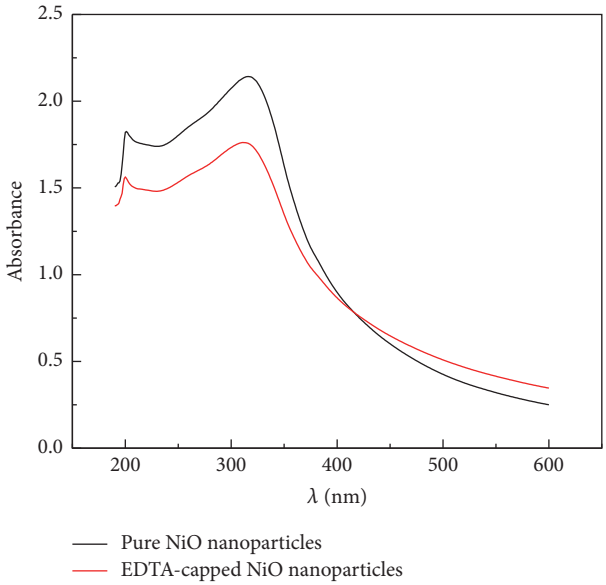

Figure 6: UV absorption spectra of pure and EDTA-capped NiO nanoparticles at 500°C.

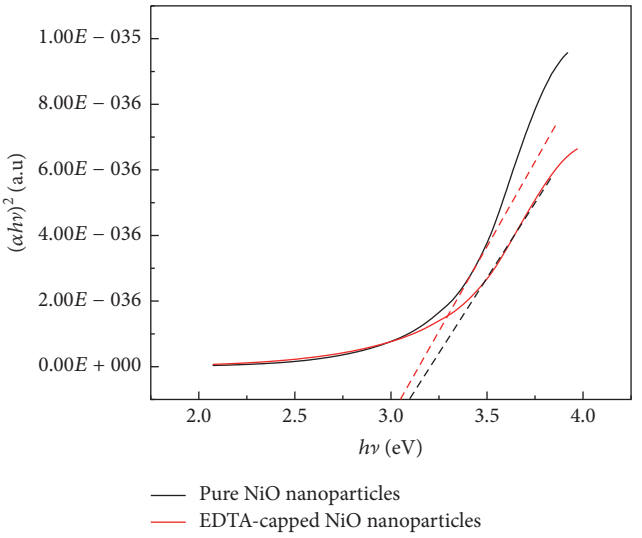

Figure 7: $(\alpha h\nu)^2$ versus photon energy of pure and EDTA-capped NiO nanoparticles.

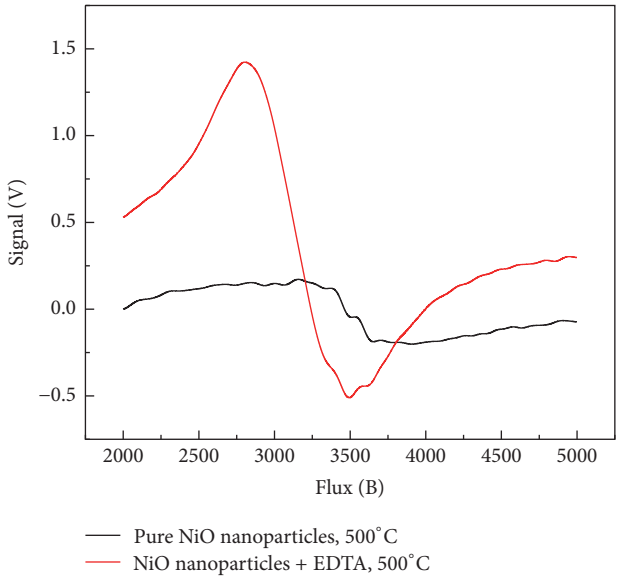

Figure 8: EPR spectra of pure and EDTA-capped NiO nanoparticles at room temperature.

nanoparticles via thermal decomposition method of nickel Schiff base complexes which results in high values of E_g.

3.7. Electron Paramagnetic Resonance. EPR spectroscopy is a useful technique for studying the materials with unpaired electrons and defects. In order to understand the effects of chelating agent EDTA on the magnetic properties of NiO nanoparticles, EPR measurement was carried out on the pure and EDTA-capped NiO nanoparticles annealed at 500°C at room temperature. EPR plots are depicted in Figure 8. It is clearly observed that pure NiO nanoparticles exhibit a broad resonance peak. The single line broad EPR spectra for these prepared NiO particles were analyzed using Lorentzian distribution function and the EPR parameters such as g-value, peak to peak line width (ΔH_{pp}), resonance field (H_r), and spin-spin relaxation time constant (T_2) were calculated and listed in Table 1. The values of g factor, the most important parameter for the description of the spin system, were calculated using the following equation [31, 32]:

$$h\nu = \Delta E = g\beta H_r, \tag{5}$$

where h is plank's constant (6.63×10^{-34} Kg·m^2·s^{-1}), ν is the microwave frequency (9.24×10^9 Hz), and β is the Bohr magnetron (9.274×10^{-28} J·G^{-1}).

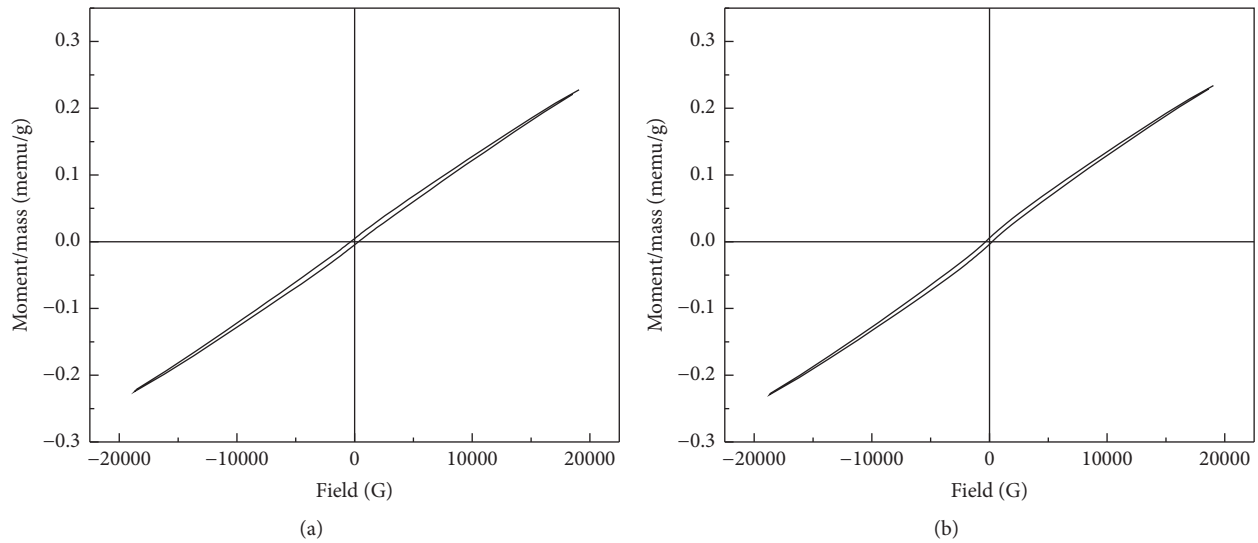

Figure 9: M–H loops for pure (a) and EDTA-capped NiO nanoparticles (b) at room temperature.

The spin-spin relaxation time constant is determined from the following equations [33]:

$$\frac{1}{T_2} = \frac{(g\beta\Delta H_{1/2})}{\hbar}$$
$$\Delta H_{1/2} = \sqrt{3}\Delta H_{\mathrm{pp}}, \quad (6)$$

where $\Delta H_{1/2}$ is the line width at half of the absorption peak.

The g-value provides information concerning the molecular motion, the paramagnetic properties, and the symmetry of ions [34]. It is observed that g-value around 1.9–2.09 could be attributed to the Ni^{2+} ions [35]. The peak to peak line width (ΔH_{pp}) decreases with the addition of capping agent. Such decrease in ΔH_{pp} may be due to the decrease in magnetic dipolar interaction and the reduction in particle size [36]. However, the slight decrease in relaxation time with the addition of EDTA is due to the decrease in electron motion and weakening of superexchange interaction in lattice [34, 37]. The magnetization value plays a dominant role in the evaluation of the resonance field and the line width [38]. The decrease in the resonance field with the addition of capping agent EDTA may be attributed to the increase in the internal magnetic field. Hence, a low field is required for the resonance in EDTA-capped NiO nanoparticles. This result agrees with these obtained by VSM measurement.

3.8. Room Temperature Magnetic Hysteresis. Magnetization measurements of pure and EDTA-capped NiO nanoparticles performed at room temperature are shown in Figures 9(a) and 9(b). Pure and EDTA-capped NiO nanoparticles depict almost linear response to the applied magnetic field. In addition, both loops pass through the origin [39] and show antiferromagnetic behavior of NiO nanoparticles. The saturation magnetization (M_s), the remnant magnetization (M_r), the coercivity (H_c), and squareness ratio (S) ($S = M_r/M_s$) are listed in Table 1. The tabulated data show that coercivity H_c decreases with the addition of capping agent EDTA, indicating that H_c is a function of the particle size that decreases with the addition of EDTA. This variation of H_c with particle size can be explained on the basis of domain structure, critical size, and surface as well as interface anisotropy of the crystal. A crystallite will spontaneously break up into a number of domains in order to reduce the large magnetization energy if it is a single domain [40]. The ratio of the energy before and after division into domains varied as $\sqrt{d}$ [41], where d is the particle size. So the energy reduces as d decreases, which suggests that the crystallite prefers to remain with single domain behavior for quite small d. However, the magnetization, M_r and M_s, of EDTA-capped NiO nanoparticles is enhanced as compared to that of the pure NiO nanoparticles because of bonding to EDTA. Such capping recovers the surface magnetization of the nanoparticles [42]. From Table 1, it is clear that $S < 0.5$ for all samples indicating that the particles interact by magnetostatic interaction and the anisotropy decreases in crystal lattice [37, 43].

Comparing our results with those obtained by Babu et al. [11], it was found that that use of either EDTA or citric acid as capping agents controls the size of nanoparticles and prevents their agglomeration and enhances the saturation magnetization of NiO nanoparticles. However, using citric acid as a capping agent results in lower sized NiO nanoparticles (25 nm) with a ferromagnetic nature and an M_s value of 0.8 emu/g. It has been strongly concluded that the magnetic behavior of NiO nanoparticles depends upon the size of nanoparticles.

4. Conclusion

NiO nanoparticles were prepared by a low cost-effective method, the coprecipitation method. The effect of the addition of capping agent EDTA to NiO nanoparticles was studied. XRD patterns showed that NiO have a face-centered

cubic (FCC) structure of crystalline size in the range of 28–33 nm. It is clearly noted that EDTA-capped NiO nanoparticles had a smaller size than uncapped nanoparticles. Hence, the addition of 0.1 M capping agent EDTA can form a nucleation point for nanoparticles growth. The Fourier transform infrared (FTIR) spectra indicate the presence of absorption bands in the range of 402–425 cm^{-1}, which is a common feature of NiO. An EPR line with g factor ≈1.9–2 is detected for NiO nanoparticles, corresponding to Ni^{2+} ions. The magnetic hysteresis of the investigated NiO nanoparticles showed that EDTA capping recovers the surface magnetization of the nanoparticles.

Competing Interests

The authors declare that they have no competing interests.

Acknowledgments

This work was performed at Beirut Arab University (BAU) in cooperation with Alexandria University (Egypt) in the Superconductivity and Metallic Glasses Lab.

References

[1] A. Barakat, M. Al-Noaimi, M. Suleiman et al., "One step synthesis of NiO nanoparticles via solid-state thermal decomposition at low-temperature of novel aqua(2,9-dimethyl-1,10-phenanthroline)$NiCl_2$ complex," *International Journal of Molecular Sciences*, vol. 14, no. 12, pp. 23941–23954, 2013.

[2] M. Salavati-Niasari, F. Mohandes, F. Davar, M. Mazaheri, M. Monemzadeh, and N. Yavarinia, "Preparation of NiO nanoparticles from metal-organic frameworks via a solid-state decomposition route," *Inorganica Chimica Acta*, vol. 362, no. 10, pp. 3691–3697, 2009.

[3] K.-C. Liu and M. A. Anderson, "Porous nickel oxide/nickel films for electrochemical capacitors," *Journal of the Electrochemical Society*, vol. 143, no. 1, pp. 124–130, 1996.

[4] L. Xiang, X. Y. Deng, and Y. Jin, "Experimental study on synthesis of NiO nano-particles," *Scripta Materialia*, vol. 47, no. 4, pp. 219–224, 2002.

[5] S. Deki, H. Yanagimoto, S. Hiraoka, K. Akamatsu, and K. Gotoh, "NH2-terminated poly(ethylene oxide) containing nanosized NiO particles: synthesis, characterization, and structural considerations," *Chemistry of Materials*, vol. 15, no. 26, pp. 4916–4922, 2003.

[6] S.-F. Liu, C.-Y. Wu, and X.-Z. Han, "Preparation of nanoscale NiO powders by polymer-network gel process," *Chinese Journal of Inorganic Chemistry*, vol. 19, no. 6, pp. 624–626, 2003.

[7] V. Ramasamy, K. Praba, and G. Murugadoss, "Synthesis and study of optical properties of transition metals doped ZnS nanoparticles," *Spectrochimica Acta Part A: Molecular and Biomolecular Spectroscopy*, vol. 96, pp. 963–971, 2012.

[8] M. Nowsath Rifaya, T. Theivasanthi, and M. Alagar, "Chemical capping synthesis of nickel oxide nanoparticles and their characterizations studies," *Nanoscience and Nanotechnology*, vol. 2, no. 5, pp. 134–138, 2012.

[9] F. Davar, Z. Fereshteh, and M. Salavati-Niasari, "Nanoparticles Ni and NiO: synthesis, characterization and magnetic properties," *Journal of Alloys and Compounds*, vol. 476, no. 1-2, pp. 797–801, 2009.

[10] Z. Fereshteh, M. Salavati-Niasari, K. Saberyan, S. M. Hosseinpour-Mashkani, and F. Tavakoli, "Synthesis of nickel oxide nanoparticles from thermal decomposition of a new precursor," *Journal of Cluster Science*, vol. 23, no. 2, pp. 577–583, 2012.

[11] G. A. Babu, G. Ravi, M. Arivanandan, M. Navaneethan, and Y. Hayakawa, "Facile synthesis of nickel oxide nanoparticles and their structural, optical and magnetic properties," *Asian Journal of Chemistry*, vol. 25, pp. S39–S41, 2013.

[12] G. S. Harish and P. Sreedhara Reddy, "Synthesis and characterization of water soluble ZnS: Ce, Cu co-doped nanoparticles: effect of EDTA concentration," *International Journal of Science and Research*, vol. 4, no. 2, pp. 221–225, 2015.

[13] J. Jayaprakash, N. Srinivasan, and P. Chandrasekaran, "Surface modifications of CuO nanoparticles using Ethylene diamine tetra acetic acid as a capping agent by sol-gel routine," *Spectrochimica Acta—Part A: Molecular and Biomolecular Spectroscopy*, vol. 123, pp. 363–368, 2014.

[14] D. A. Reddy, G. Murali, R. P. Vijayalakshmi, and B. K. Reddy, "Room-temperature ferromagnetism in EDTA capped Cr-doped ZnS nanoparticles," *Applied Physics A*, vol. 105, no. 1, pp. 119–124, 2011.

[15] M. S. Sadjadi and A. Khalilzadegan, "The effect of capping agents, EDTA and Eg on the structure and morphology of CdS nanoparticles," *Journal of Non-Oxide Glasses*, vol. 7, no. 4, pp. 55–63, 2015.

[16] H. F. Devi and T. D. Singh, "Comparison on effect of EDTA and citrate mediated on luminescence property of Eu^{3+} doped YPO_4 nanoparticles," *Perspectives in Science*, vol. 8, pp. 267–269, 2016.

[17] A. Rahdar, M. Aliahmad, and Y. Azizi, "NiO nanoparticles: synthesis and characterization," *Journal of Nanostructures*, vol. 5, no. 2, pp. 145–151, 2015.

[18] M. Kanthimathi, A. Dhathathreyan, and B. U. Nair, "Nanosized nickel oxide using bovine serum albumin as template," *Materials Letters*, vol. 58, no. 22-23, pp. 2914–2917, 2004.

[19] M. A. Gondal, T. A. Saleh, and Q. A. Drmosh, "Synthesis of nickel oxide nanoparticles using pulsed laser ablation in liquids and their optical characterization," *Applied Surface Science*, vol. 258, no. 18, pp. 6982–6986, 2012.

[20] C. Suryanarayana and N. M. Grant, *A Practical Approach*, Plenum Press, New York, NY, USA, 1998.

[21] X. Shi, J. Wang, and X. Cai, "Effects of EDTA and boric acid on the morphology of $CaCO_3$ particles," *Journal of Nanomaterials*, vol. 2012, Article ID 532847, 2012.

[22] Y. Mahaleh, S. K. Sadrnezhaad, and D. Hosseini, "NiO nanoparticles synthesis by chemical precipitation and effect of applied surfactant on distribution of particle size," *Journal of Nanomaterials*, vol. 2008, Article ID 470595, 4 pages, 2008.

[23] R. Javed, M. Usman, S. Tabassum, and M. Zia, "Effect of capping agents: structural, optical and biological properties of ZnO nanoparticles," *Applied Surface Science*, vol. 386, pp. 319–326, 2016.

[24] A. D. Khalaji, "Preparation and characterization of NiO nanoparticles via solid-state thermal decomposition of nickel (II) Schiff base complexes [Ni (salophen)] and [Ni (Me-salophen)]," *Journal of Cluster Science*, vol. 24, no. 1, pp. 209–215, 2013.

[25] Z. Wei, H. Qiao, H. Yang, L. Zhu, and X. Yan, "Preparation and characterization of NiO nanoparticles by anodic arc plasma method," *Journal of Nanomaterials*, vol. 2009, Article ID 795928, 5 pages, 2009.

[26] M. Salavati-Niasari, N. Mir, and F. Davar, "A novel precursor in preparation and characterization of nickel oxide nanoparticles via thermal decomposition approach," *Journal of Alloys and Compounds*, vol. 493, no. 1-2, pp. 163–168, 2010.

[27] M. Sharma, S. Kumar, and O. P. Pandey, "Study of energy transfer from capping agents to intrinsic vacancies/defects in passivated ZnS nanoparticles," *Journal of Nanoparticle Research*, vol. 12, no. 7, pp. 2655–2666, 2010.

[28] B. Dong, L. Cao, G. Su, W. Liu, H. Qu, and H. Zhai, "Water-soluble ZnS:Mn/ZnS core/shell nanoparticles prepared by a novel two-step method," *Journal of Alloys and Compounds*, vol. 492, no. 1-2, pp. 363–367, 2010.

[29] D. Lincot and G. Hodes, *Chemical Solution Deposition of Semiconducting and Non-Metallic Films: Proceedings of the International Symposium*, The Electrochemical Society, 2006.

[30] A. D. Khalaji and D. Das, "Synthesis and characterizations of NiO nanoparticles via solid-state thermal decomposition of nickel (II) Schiff base complexes," *International Nano Letters*, vol. 4, no. 3, pp. 1–5, 2014.

[31] D. M. Murphy, "EPR (Electron Paramagnetic Resonance) spectroscopy of polycrystalline oxide systems," *ChemInform*, vol. 41, no. 13, pp. 1–10, 2010.

[32] A. Abragam and B. Bleaney, *Electron Paramagnetic Resonance of Transition Ions*, OUP, Oxford, UK, 2012.

[33] N. Yadav, A. Kumar, P. S. Rana, D. S. Rana, M. Arora, and R. P. Pant, "Finite size effect on Sm^{3+} doped $Mn_{0.5}Zn_{0.5}Sm_x\ Fe_{2-x}O_4$ ($0 \leq x \leq 0.5$) ferrite nanoparticles," *Ceramics International*, vol. 41, no. 7, pp. 8623–8629, 2015.

[34] G. S. Shahane, A. Kumar, M. Arora, R. P. Pant, and K. Lal, "Synthesis and characterization of Ni-Zn ferrite nanoparticles," *Journal of Magnetism and Magnetic Materials*, vol. 322, no. 8, pp. 1015–1019, 2010.

[35] A. Perumal Bhagaban Kisan, P. Ravikumar, A. Das, and A. Srinivasan, "vibrational, optical and magnetic properties of NiO nanoparticles," *Journal of Nanoscience Letters*, vol. 4, article 160, 2015.

[36] A. Kumar, P. S. Rana, M. S. Yadav, and R. P. Pant, "Effect of Gd^{3+} ion distribution on structural and magnetic properties in nano-sized Mn-Zn ferrite particles," *Ceramics International*, vol. 41, no. 1, pp. 1297–1302, 2015.

[37] D. E. Bakeer, A. I. Abou-Aly, N. H. Mohammed, R. Awad, and M. Hasebbo, "Characterization and Magnetic properties of nanoferrite $ZnFe_{2-x}La_xO_4$ prepared by co-precipitation method," *Journal of Superconductivity and Novel Magnetism*, pp. 1–10, 2016.

[38] S. C. Byeon, K. S. Hong, and I.-T. Kim, "Line width of manganese-zinc ferrite polycrystals with oxygen partial pressure," *Journal of Applied Physics*, vol. 83, no. 11, pp. 6873–6875, 1998.

[39] P. Ravikumar, B. Kisan, and A. Perumal, "Enhanced room temperature ferromagnetism in antiferromagnetic NiO nanoparticles," *AIP Advances*, vol. 5, no. 8, Article ID 087116, 2015.

[40] M. Zhang, Z. Zi, Q. Liu et al., "Size effects on magnetic properties of prepared by sol-gel method," *Advances in Materials Science and Engineering*, vol. 2013, Article ID 609819, 10 pages, 2013.

[41] M. George, A. Mary John, S. S. Nair, P. A. Joy, and M. R. Anantharaman, "Finite size effects on the structural and magnetic properties of sol-gel synthesized $NiFe_2O_4$ powders," *Journal of Magnetism and Magnetic Materials*, vol. 302, no. 1, pp. 190–195, 2006.

[42] B. Andrzejewski, W. Bednarski, M. Kaźmierczak et al., "Magnetization enhancement in magnetite nanoparticles capped with alginic acid," *Composites Part B: Engineering*, vol. 64, pp. 147–154, 2014.

[43] E. C. Stoner and E. P. Wohlfarth, "A mechanism of magnetic hysteresis in heterogeneous alloys," *Philosophical Transactions of the Royal Society A: Mathematical, Physical and Engineering Sciences*, vol. 240, no. 826, pp. 599–642, 1948.